



UMERC+METS 2024 Conference

7-9 August | Duluth, MN, USA

Geometry Optimization of Cable-Based Actuation for Small-Scale Model Testing of a Floating Marine Turbine

Anisha Sharma^a, Matthew Hall^b, Hannah Ross^b, Kathryn Johnson^{b,c}, Will Wiley^b, Senu Srinivas^b

^aMines/NREL Advanced Energy Systems Graduate Program, Colorado School of Mines

^bNational Renewable Energy Laboratory (NREL), Golden CO

^cElectrical Engineering Department, Colorado School of Mines

Abstract

This research aims to apply combined wave and tidal current loads to a small-scale floating marine current turbine in a wave tank, where an actuation system applies hydrodynamic and mooring forces on the floating platform based on results from a simulation. We use a real-time hybrid model test setup with physical wave forcing from the wave tank and simulated current and mooring forces implemented through a tensioned cable array. For this paper, we developed an optimization algorithm that adjusts the geometry of the cable array to achieve more efficient tension allocation across the cables for the loads that need to be actuated. By adjusting the points where the cables are attached to the floating platform and the angles between the platform and the winches, an optimal cable geometry can be found to minimize tension variations in the lines, maintain the desired pretension, and prevent excessive tensions. We present the optimization problem formulation, the actuation system evaluation approach, and optimization results that show effective cable actuation setups that are being considered for implementation in the wave tank tests.

Keywords: optimization, real-time hybrid model testing, cable-based actuation, experimental testing, floating marine turbine

1. Introduction

Floating offshore structures must withstand harsh environments. To better model these structures under the influence of combined current-wind-wave loading, small-scale model testing in a wave basin can be used as part of the design process. The purpose of such testing is to understand how the structures will behave under a range of environmental conditions and to characterize the coupled dynamic response of the whole system. Traditional small-scale testing comes with some inherent challenges. While the key fluid-structure interactions are fairly well understood, they are governed by two different nondimensional parameters: the Reynolds number quantifies the importance of inertial forces over viscous forces in the flow while the Froude number describes open channel flow regimes. To correctly scale the model, the goal is to maintain the same Froude and Reynolds numbers on the small-scale test vessel as on the full-scale system. However, correct scaling of one parameter yields inaccurate forces from the other [1].

There are also equipment limitations in test facilities. It is difficult to create open-ocean conditions without sophisticated equipment. Thus, some environmental loads must often be applied via other means. This difficulty has inspired hybrid model testing where actuator systems are used to mimic effects not physically captured in experiments. These systems vary in type of actuation. For example, Otter et al. designed a multi-propellor device to emulate the effects of wind flow on a floating wind turbine using a set of aerial drone propellers [1]. Vilsen et al. designed a hybrid model test involving a physical substructure of a cylindrical buoy attached to actuation lines with

load cells and markers to measure movement. A numerical substructure consisted of a model that computed the expected loads with a reference feed-forward controller and applied those loads to the physical substructure [2].

In this work, a cable-based actuation system will be used in conjunction with a numerical submodel to calculate expected loads. The floating marine turbine tested in the wave basin will be attached to a cable array, which will apply numerically calculated loads from a turbine simulation software.

1.1. Hybrid Submodeling Strategy

The hybrid test is composed of two submodels: numerical and physical, as depicted in Figure 1. The physical submodel consists of the small-scale marine turbine. In this work, we test the floating RM1 marine energy turbine [3] in a wave basin. The model is connected to an array of tensioned cables attached to winch-pulley systems. The numerical submodel consists of OpenFAST, an open-source wind and marine turbine simulation tool [4], that numerically calculates the expected loads given the environmental conditions and test articles displacements. The force configuration output by OpenFAST, called a wrench force, is converted to cable array tensions that are actuated by the winch-pulleys. A controller connects the two subsystems and ensures the correct tensions are actuated by each cable. The measurement system consists of an optical tracking system that records the current position and orientation of the platform and load cells that measure the tension in the cables. Figure 1 shows the overall setup of the sensors, the platform in the wave tank, and the expected interactions between the components.

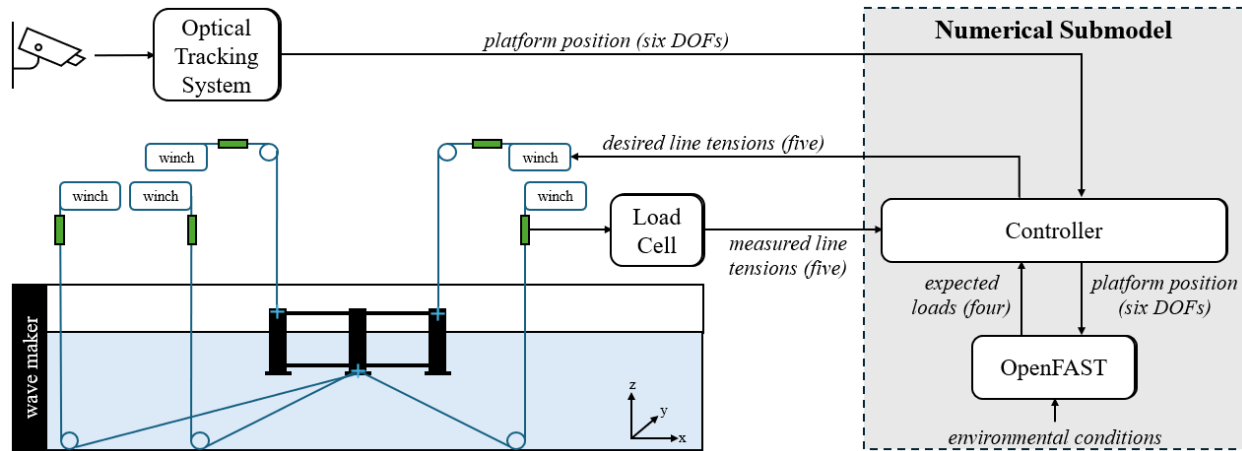


Figure 1. Overview of numerical and physical submodels. Green boxes represent load cells. Only one feedback loop has been drawn to avoid cluttering the image, but each load cell has its own feedback path to the controller.

1.2. Cable Array and Actuation System

For the planned experiments, we model forces in four degrees of freedom (DOFs): F_x , F_y , F_z , and M_y (force in surge, sway, and heave directions and moment in pitch direction, respectively), which were identified as the dominating forces in previous simulations. To actuate four DOFs with non-rigid cables, five cables are needed to ensure that adequate tensions are maintained because each cable must be pretensioned to ensure it does not go slack. To efficiently actuate the desired forces, tension allocation algorithms can be used to distribute the summed force across multiple cables. These algorithms apply the required forces while distributing tension in a way that minimizes the load variations in the lines while maintaining the desired level of pretension and preventing excessive line tensions.

The wrench vector of expected forces, \mathbf{w} , which is generated by the numerical model, consists of the three forces and one moment. A structure matrix, \mathbf{A}^T , is derived from the geometry of the cable array and the cable coupling points to the physical structure and defined by the Jacobian of cable lengths with respect to time. Equation (1) relates the structure matrix and the wrench vector to a vector, $\boldsymbol{\tau}$, of line tensions for all five cables.

$$\mathbf{w} = -\mathbf{A}^T \boldsymbol{\tau} \quad (1)$$

Since \mathbf{A}^T is not a square matrix, to solve for the required tension vector, $\boldsymbol{\tau}$, the Moore-Penrose pseudo-inverse of the structure matrix can be used, resulting in the final tension vector formulation in Equation (2) [5].

$$\boldsymbol{\tau} = -\mathbf{A}^{+T}\mathbf{w} + \boldsymbol{\tau}_m - \mathbf{A}^{+T}\mathbf{A}^T\boldsymbol{\tau}_m = \begin{bmatrix} T_1 \\ \dots \\ T_5 \end{bmatrix} \quad (2)$$

where \mathbf{A}^{+T} is the Moore-Penrose pseudo-inverse, $\boldsymbol{\tau}_m$ is a vector whose elements are the desired mean tension value for all five cables, and T_{1-5} are the tension values in the five cables.

2. Methodology for Optimizer Development

2.1. Overall Approach

This work focuses on developing an optimization algorithm that tunes the cable geometry to achieve more efficient force actuation. The two variables that govern the cable geometry are (1) where the cables are attached to pulley wheels (small circles in Figure 1) that route to on-land winch actuators and (2) the coupling points where the cables are attached to the floating platform (indicated by '+' in Figure 1). Both affect the angle between the cable and the platform. An optimal cable geometry can be found given the expected loading by adjusting those values. By optimizing the cable geometry rather than simply choosing convenient locations for coupling points and pulleys, the cable system can more effectively actuate the desired loads. Figure 2 shows the overall optimization scheme where the optimizer starts with an initial guess for the pulley locations and calculates the deviation from a mean tension value.

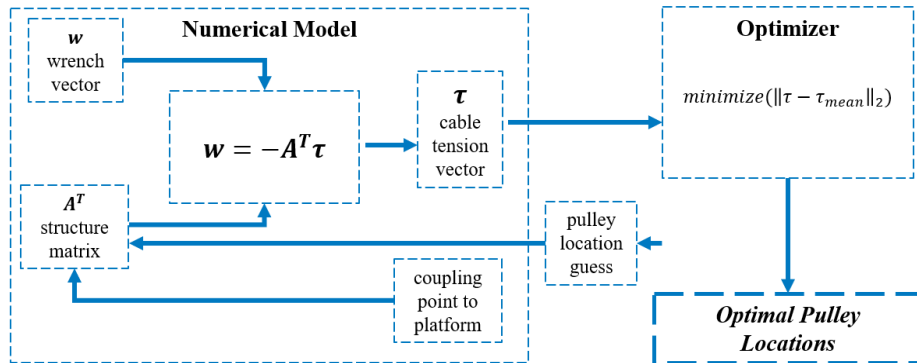


Figure 2. Schematic of Optimization Method

2.2. Implementation

The decision variables the optimizer is adjusting are the x, y, and z coordinates of all five pulley wheels. They are constrained such that the pulleys stay within the boundaries of the wave basin dimensions to prevent any cables from needing to be routed through the wave tank walls. Given the no-slack condition of the cable array within the optimization, the tension values are also constrained such that no tension falls below zero. The objective function is the L2 norm of the deviation of line tensions from the mean tension value. The optimization method was set up using the Python SciPy library for constrained optimization. Given the nature of the constraints and that the gradient of the objective function is difficult to compute, the Constrained Optimization by Linear Approximations (COBYLA) optimization method [6] was used to compute optimal pulley locations. We selected the test scenario expected to generate the highest loads on the system to determine the wrench vectors. The optimizer was run for 14 different coupling point configurations, and the results were compared to ascertain the optimal anchor and coupling point combination.

3. Results

The goal of the optimization was to distribute the load variations somewhat more evenly across the five lines as well as maintain the desired level of pretension and prevent excessive line tensions. We started with a base

configuration seen in Figure 3(a) with the lower-line coupling points centered on the platform's base and the upper lines attached at the platform's edges. We then tested an additional 14 variations of the coupling points. The coupling points were chosen based on which points could easily have cables attached and to ensure a variety in the coupling point configurations tested. Based on the tension ranges for each line as well as the overall tension needed for each optimized configuration compared to the standard control, we chose two geometries that seemed to best allocate tension, shown in Figure 3. A few other geometries performed similarly well, but the two chosen were best at minimizing the overall tension range necessary as well as distributing somewhat evenly over each line. Optimized

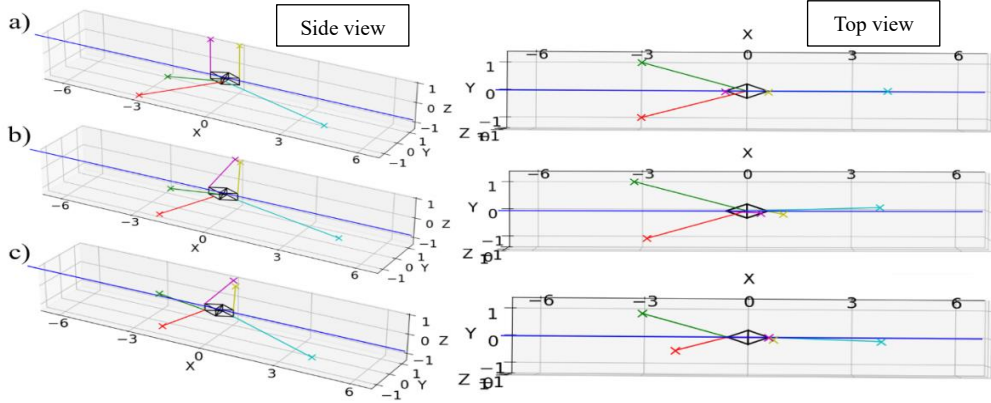


Figure 4. a) Base configuration, b) optimized geometry 2 (G2), and c) optimized geometry 4 (G4). Black lines represent the platform, Xs represent the pulleys, the five color lines represent the five cables, and the grid border is representative of the wave tank dimensions

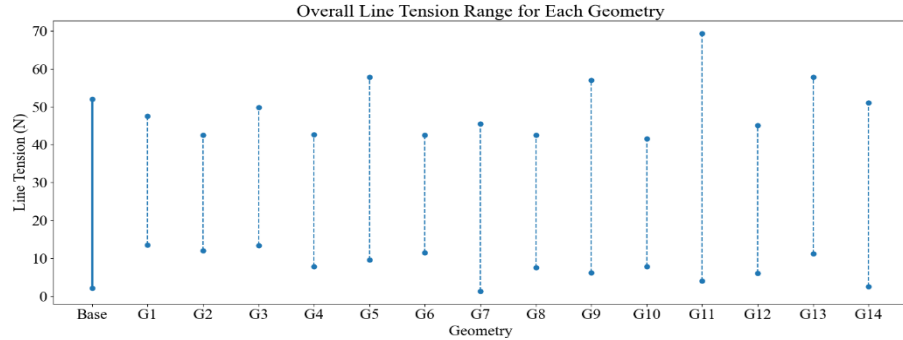


Figure 3. Tension ranges for each geometry showing the minimum and maximum across all five lines geometry 2 ("G2," Figure 3(b)) has the lower lines at the tips of the platform while geometry 4 ("G4," Figure 3(c)) has the lower lines attached halfway to the edges. Figure 4 shows the maximum and minimum tension for each of the optimized geometries and the base configuration.

To understand the results of our optimization, we examined time series for many of the cases summarized in Figure 4. Figure 5 plots the series plot of the required wrench force for a single load case and the corresponding line tensions needed to actuate that force for the base geometry and geometries 2 and 4. As seen in Figure 5, the optimized configurations successfully center the line tensions around a mean value of approximately 30 N, whereas the base case has some cables tensioned much more than others. For example, line 3 (pointing downstream) sees high tensions since the force along that axis is larger in the wrench force configuration. Line 4 also sees high tensions because the lower lines (which are coupled at the center of the model) cannot contribute as significantly to the pitch moment. Both optimized geometries have the upper two lines angled inward to help actuate the high F_x force. The optimized geometries also have the lower lines farther out from each other so they can contribute better to the desired pitch moment. By shifting the pulley locations and coupling points to create this optimized geometry, we can more effectively allocate the forces to all five cables and avoid tension spikes and high internal load variations. With these changes, the tension range in the upper lines was reduced from 40.77 N in the base configuration to 17.73 N and 22.61 N in G2 and G4, respectively. Similarly, the tension range in the lower lines was reduced from 43.26 N to 30.41 N and 32.47 N, respectively. Overall, the tension range actuated through the lines was reduced by 19.45 and 15.01 N in G2 and G4, respectively.

The tension allocation results show that our optimization method can select cable geometry configurations to more effectively distribute the tension throughout the cable array and avoid tension spikes compared to the base configuration. However, there is a trade-off to consider between the complexity of the design and the reduced actuation requirements. For example, both G2 and G4 require the lower pulleys to be lifted off the wave basin floor using supporting structures, which may add unnecessary instability and complexity to the design. Both optimized designs also require the upper two lines to be angled inward, creating a risk of line entanglement if the platform experiences a larger yaw movement. Given these considerations, the optimizer is a good place to investigate possible designs, but it may be useful to further refine the constraints and consider whether the added complexity will significantly improve the final tension allocation. When fabricating the actual system, some coupling points might also be more structurally sound to attach cables to, which is another consideration while deciding on the final geometry. Running an optimization and examining multiple geometries is also helpful to establish patterns between the different configurations and use those results in the final design.

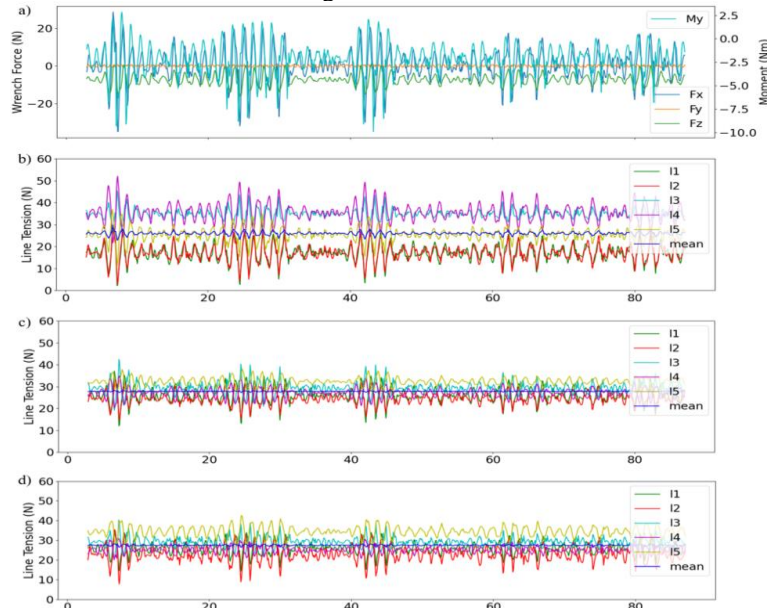


Figure 5. Time series of a) wrench force used for all cases, b-d) line tensions for base geometry, geometry 2, and geometry 4, respectively

4. Conclusion

Our optimization results show significantly better tension allocation than the baseline cable geometry we started with. Using this method ensures that the winch-and-pulley system is working effectively and reduces sharp spikes in tension and high internal load variations, which can help prevent mechanical issues and snap loads, protecting the entire hybrid system. By reducing the maximum tension value, we can also avoid high costs associated with large winch units and we can appropriately size the actuators.

Acknowledgements

This work was authored in part by the National Renewable Energy Laboratory, operated by Alliance for Sustainable Energy, LLC, for the U.S. Department of Energy (DOE) under Contract No. DE-AC36-08GO28308. Funding provided by the U.S. Department of Energy Office of Energy Efficiency and Renewable Energy Water Power Technologies Office Powering the Blue Economy Fundamental Research and Development program. The views expressed in the article do not necessarily represent the views of the DOE or the U.S. Government. The U.S. Government retains and the publisher, by accepting the article for publication, acknowledges that the U.S. Government retains a nonexclusive, paid-up, irrevocable, worldwide license to publish or reproduce the published form of this work, or allow others to do so, for U.S. Government purposes. This work is supported by Colorado

School of Mines and National Renewable Energy Laboratory Advanced Energy Systems Graduate Program,
Colorado School of Mines, Golden CO 80401, USA.

References

- [1] Otter, A., Murphy, J., & Desmond, C. J. (2020). Emulating aerodynamic forces and moments for hybrid testing of floating wind turbine models. *Journal of Physics: Conference Series*, 1618(3), 032022.
<https://doi.org/10.1088/1742-6596/1618/3/032022>
- [2] Vilsen, S. A., Sauder, T., & Sørensen, A. J. (2017). Real-Time Hybrid Model Testing of Moored Floating Structures Using Nonlinear Finite Element Simulations. In M. S. Allen, R. L. Mayes, & D. J. Rixen (Eds.), *Dynamics of Coupled Structures*, Volume 4 (pp. 79–92). Springer International Publishing.
https://doi.org/10.1007/978-3-319-54930-9_8
- [3] Wiley, W., Ross, H., Sundarajan, A. K., & Tran, T. T. (2023). Design and Modeling of an Open-Source Baseline Floating Marine Turbine. *Renewable Energy*.
- [4] OpenFAST. (n.d.). Retrieved March 28, 2024, from <https://www.nrel.gov/wind/nwtc/openfast.html>
- [5] Hall, M. (2016). Hybrid Modeling of Floating Wind Turbines [The University of Maine].
<https://digitalcommons.library.umaine.edu/etd/2477>